A synthetic perturbative hypothesis for the multiscale analysis of the wake instability

A synthetic perturbative hypothesis for multiscale analysis of convective wake instability

D. Tordella
Dipartimento di Ingegneria Aeronautica e Spaziale, Politecnico di Torino, Torino 10129, Italy

S. Scarsoglio
Scuola di Dottorato, Politecnico di Torino, Torino 10129, Italy

M. Belan
Dipartimento di Ingegneria Aeronautica e Spaziale, Politecnico di Milano, Milano 20156, Italy

(Received 3 January 2006; accepted 5 April 2006; published online 11 May 2006)

The paper presents a nonparallel stability analysis of the intermediate region of the two-dimensional wake behind a bluff body. In particular, it analyzes the convective instabilities using a Wentzel-Kramers-Brillouin-Jeffreys method on a basic flow previously derived from intermediate asymptotics [D. Tordella and M. Belan, Phys. Fluids **15**, 1897 (2003)]. The multiscaling is carried out to explicitly account for the effects associated to the lateral momentum dynamics at a given Reynolds number. These effects are an important feature of the base flow and are included in the perturbative equation as well as in the associated modulation equation. At the first order in the multiscaling, the disturbance is locally tuned to the property of the instability, as can be seen in the zero-order theory (near-parallel parametric Orr-Sommerfeld treatment). This leads to a synthetic analysis of the nonparallel correction of the instability characteristics. The system is, in fact, considered to be locally perturbed by waves with a wave number that varies along the intermediate wake and which is equal to the wave number of the dominant saddle point of the zero order dispersion relation, taken at different Reynolds numbers. In this study, the Reynolds number is thus the only parameter. It is shown that the corrections to the frequency, and to the temporal and spatial growth rates are remarkable in the first part of the intermediate wake and lead to absolute instability in regions that extend to about ten body scales. The correction increases with the Reynolds number and agrees with data from laboratory and numerical experiments in literature. An eigenfunction and eigenvalue asymptotic analysis for the far wake is included, which is in excellent agreement with the complete problem. © *2006 American Institute of Physics*. [DOI: 10.1063/1.2201114]

I. INTRODUCTION

A two-dimensional (2D) wake behind a stationary cylinder is a spatially developing flow in which self-sustained oscillations occur.[1–6] The unsteady flow is modeled as viscous and incompressible. The disturbances grow linearly in a region of absolute instability that exists downstream to the back stagnation point or trailing edge of the body that generates the wake. This region is either preceded or followed by a convectively unstable region.[7–10] The perturbation saturates in the absolutely unstable region and tunes to a frequency that corresponds to a global mode, which in literature is selected according to criteria that are usually associated to the dominant saddle points of the local dispersion relation.[11,12] The linear global mode has a nonlinear counterpart, which stems from the extension of the linear concepts to the nonlinear context.[13]

In a stability analysis, the disturbance is superimposed onto the laminar field, which is usually assumed to be locally parallel. The analysis is then decomposed into a sequence of equivalent parallel problems: the properties of the wake, at each section behind the cylinder, are represented by the stability properties of a parallel flow with the same average velocity profile.[2,4,14] This is a restrictive assumption, since it underestimates the effects associated to the lateral convection in the basic flow. In fact, in so doing, the lateral convection is not directly present in both the base flow and the perturbative equations. When the flow divergence is slow compared to the disturbance quantities the structure of the governing equations allows the nonparallel effects to be incorporated with a perturbation approach based on multiple-scale analysis. Two scales are usually considered: a long scale, that is, the scale of the mean flow variations, and a short scale, the scale over which the disturbances vary. At the first order, the multiscaling allows a differential equation to be written for the wave modulation, which in turn yields the correction on the stability characteristics. If the multiscaling is limited to the spatial variable, the modulation equation is ordinary and gives the correction for the complex wave number.[15,16] If the multiscaling is both spatial and temporal, the modulation equation is a partial differential equation that gives a correction of the complex frequency and wave number (see, for instance, Bouthier[17] for an application to boundary layer instability).

In this paper, a spatio-temporal multiscaling approach is applied to the intermediate asymptotics[18] of the cylinder wake, where the instability in the quasiparallel approximation is convective. The two-dimensional stability analysis is restricted from critical to Reynolds number 160, since for

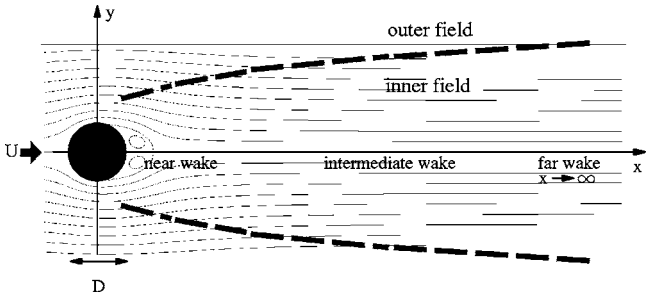

FIG. 1. Sketch of the laminar wake flow behind a 2D bluff body.

large three-dimensional disturbances have to be considered. The basic flow is represented by an accurate analytical expansion solution that explicitly represents the lateral convection dynamics.[19,20] This solution accounts for longitudinal and lateral convection and diffusion and is obtained by matching the vorticity, entrainment (lateral) velocity, and pressure gradient of quasisimilar inner and outer Navier-Stokes solutions (Sec. II A). The multiscaling is applied to the stability analysis (Sec. II B). The disturbance can be considered, in a synthetic way, as a variable wave, which corresponds in each longitudinal section to the more unstable mode; that is, to a wave with wave number equal to that of the dominant saddle point of the dispersion relation. This allows the streamwise slow variation to be at once incorporated into the coefficients of the modulation equation, which is thus only parametrized with respect to the Reynolds number (Sec. II C). This results in the determination of the complex wave modulation and downstream distribution of the (order zero+order 1) characteristics values associated to the dominant saddle point of each intermediate wake section. Section III describes the obtained results, in particular the appearance of absolute instability regions in the first part of the intermediate wake, and offers a comparison with global data from numerical and laboratory stability studies.[3,10,21] An asymptotic analysis of the far wake is then proposed in Sec. IV. This analysis offers *a priori* inferences that agree with the far field results obtained from the numerical integration of the modulation equation. Detailed extrapolations of the downstream distribution of the instability characteristics of the dominant saddle points at order zero are given in the Appendix.

II. MULTISCALE ANALYSIS

A. Base flow

An approximated Navier-Stokes solution for the intermediate region of the two-dimensional steady bluff body wake has been considered (see Fig. 1). In this intermediate region between the near wake, which includes the two symmetrical counter-rotating eddies, and the ultimate far wake, the lateral momentum dynamics is not yet negligible. The assumption of the existence of an intermediate wake region introduces a differentiation between intermediate asymptotics and infinite asymptotics. It also allows the thin shear layer hypothesis and relevant near-similar variable transformations to be adopted for the inner flow. The analytical solution used here accounts for the effects of the streamwise diffusion, nonlinear convection and entrainment at the lower orders and for the pressure gradient and linear and nonlinear exchange of vorticity from the inner towards the outer part of the flow at higher orders.[19,20] The previously mentioned lower order effects are considered in the primary flow representation through a multiscale analysis which, from the first order in ϵ, explicitly introduces the transversal momentum component of the basic flow. The solution is obtained by matching an inner solution—a Navier-Stokes expansion in powers of the inverse of the longitudinal coordinate $(x^{-n/2}, n=0,1,2,\ldots)$—and an outer solution, which is a Navier-Stokes asymptotic expansion in powers of the inverse of the distance from the body. The physical quantities involved in matching criteria are the vorticity, the longitudinal pressure gradients generated by the flow and the entrainment velocities. The lateral decay results to be algebraic at high orders in the inner expansion solution. Assuming the inner expansion up to $O(x^{-3/2})$ as being an approximation of the primary wake flow and using the quasisimilar transformation

$$x = x, \quad \eta = x^{-1/2} y, \tag{1}$$

where (x,y) are the adimensional longitudinal and normal coordinates, the adimensional velocity components (u,v) can be written as

$$u = 1 + x^{-1/2}\phi_1(\eta) + x^{-1}\phi_2(\eta) + x^{-3/2}\phi_3(\eta), \tag{2}$$

$$v = x^{-1}\chi_2(\eta) + x^{-3/2}\chi_3(\eta). \tag{3}$$

The physical quantities involved in the adimensionalization are the length D of the body that generates the wake, the density ρ and the velocity U of the free stream. The Reynolds number is defined as $\mathrm{R}=\rho UD/\mu$, where μ is the dynamic viscosity of the fluid. According to the multiscale approach, the slow spatial and temporal variables are

$$x_1 = \varepsilon x, \quad t_1 = \varepsilon t, \tag{4}$$

where $\varepsilon = 1/\mathrm{R}$. Since $\eta = (\mathrm{R}x_1)^{-1/2} y$, the velocity components of the basic flow can also be written as

$$u = \partial_y \Psi = u_0(x_1, y) + \varepsilon u_1(x_1, y) + \cdots, \tag{5}$$

$$v = -\partial_x \Psi = -\varepsilon \partial_{x_1} \Psi = \varepsilon v_1(x_1, y) + \cdots. \tag{6}$$

By only considering the integer powers of ε up to the first order, Eqs. (2) and (3) can assume the multiscale structure (5) and (6). For the u component, it results that

$$\begin{aligned} u &= 1 + \mathrm{R}^{-1/2} x_1^{-1/2} \phi_1(y/\sqrt{\mathrm{R}x_1}) + \mathrm{R}^{-1} x_1^{-1} \phi_2(y/\sqrt{\mathrm{R}x_1}) \\ &\quad + \mathrm{R}^{-3/2} x_1^{-3/2} \phi_3(y/\sqrt{\mathrm{R}x_1}) \\ &= [1 + \mathrm{R}^{-1/2} x_1^{-1/2} \phi_1(\eta)] + \varepsilon [x_1^{-1} \phi_2(\eta) \\ &\quad + \mathrm{R}^{-1/2} x_1^{-3/2} \phi_3(\eta)], \end{aligned} \tag{7}$$

so that

$$u_0 = 1 + \mathrm{R}^{-1/2} x_1^{-1/2} \phi_1 = 1 - x_1^{-1/2} \mathrm{R}^{-1/2} \tilde{c_D} C_1 e^{-(\mathrm{R}\eta^2)/4}, \tag{8}$$

$$u_1 = x_1^{-1}\phi_2 + \mathrm{R}^{-1/2}x_1^{-3/2}\phi_3$$
$$= -x_1^{-1}\frac{\tilde{c_D}^2}{2}e^{-(\mathrm{R}\eta^2)/4}\left\{C_2\,{}_1\mathrm{F}_1\left(-\frac{1}{2},\frac{1}{2};\frac{\mathrm{R}}{4}\eta^2\right) + e^{-(\mathrm{R}\eta^2)/4} + \frac{\sqrt{\pi\mathrm{R}}}{2}\eta\,\mathrm{erf}\left(\frac{\sqrt{\mathrm{R}}}{2}\eta\right)\right\} - x_1^{-3/2}\mathrm{R}^{-1/2}\tilde{c_D}^3(\mathrm{R}\eta^2-2)$$
$$\times \mathrm{e}^{-(\mathrm{R}\eta^2)/4}\left[\frac{1}{2}C_3 - \mathrm{R}F_3(\eta)\right], \tag{9}$$

where $C_1=1$, constants C_2 and C_3 are integration constants that depend on the Reynolds number,[20] while constant $\tilde{c_D}$ is related to the drag coefficient $\left[\tilde{c_D}=\frac{1}{4}(\mathrm{R}/\pi)^{1/2}c_D(\mathrm{R})\right]$. Function ${}_1\mathrm{F}_1$ is the confluent hypergeometric function and F_3 is the particular case, for $n=3$, of the general nth-order function

$$F_n(\eta) = \int_0^\eta \frac{e^{(\mathrm{R}\eta^2)/4}}{\mathrm{Hr}_{n-1}^2(\eta)}G_n(\eta)\mathrm{d}\eta,$$

$$G_n(\eta) = \tilde{c_D}^{-n}\int_0^\eta M_n(\eta)\mathrm{Hr}_{n-1}(\eta)\mathrm{d}\eta,$$

where $\mathrm{Hr}_{n-1}(\eta)=\mathrm{H}_{n-1}(\frac{1}{2}\mathrm{R}^{1/2}\eta)$ (H_n are Hermite polynomials). Function $M_n(\eta)$ is the sum of the nonhomogeneous terms of the general ordinary differential equation for ϕ_n, $n\geqslant 1$, obtained from the x component of the Navier-Stokes equation.[19] Function M_n includes the effects of the streamwise pressure gradient and diffusion terms and also of part of the longitudinal convection term.

At the same approximation order, the v component is given by

$$v = \mathrm{R}^{-1}x_1^{-1}\chi_2(x_1,y) + \mathrm{R}^{-3/2}x_1^{-3/2}\chi_3(x_1,y)$$
$$= \varepsilon[x_1^{-1}\chi_2(\eta) + \mathrm{R}^{-1/2}x_1^{-3/2}\chi_3(\eta)] \tag{10}$$

so that

$$v_1 = x_1^{-1}\chi_2 + x_1^{-3/2}\mathrm{R}^{-1/2}\chi_3$$
$$= x_1^{-1}\frac{\tilde{c_D}}{2}\eta e^{-(\mathrm{R}\eta^2)/4} + x_1^{-3/2}\mathrm{R}^{-1/2}\frac{\tilde{c_D}^2}{2}$$
$$\times\left\{C_2\left[-\frac{1}{2}\int e^{-(\mathrm{R}\eta^2)/4}\,{}_1\mathrm{F}_1\left(-\frac{1}{2},\frac{1}{2};\frac{\mathrm{R}}{4}\eta^2\right)\mathrm{d}\eta - \frac{1}{2}\eta e^{-(\mathrm{R}\eta^2)/4}\,{}_1\mathrm{F}_1\left(-\frac{1}{2},\frac{1}{2};\frac{\mathrm{R}}{4}\eta^2\right)\right] - \frac{1}{2}\eta e^{-(\mathrm{R}\eta^2)/2} - \sqrt{\frac{\pi}{2\mathrm{R}}}\,\mathrm{erf}\left(\sqrt{\frac{\mathrm{R}}{2}}\eta\right) + \left(\frac{1}{2}\sqrt{\frac{\pi}{\mathrm{R}}} - \frac{\sqrt{\pi\mathrm{R}}}{4}\eta^2\right)e^{-(\mathrm{R}\eta^2)/4}\mathrm{erf}\left(\frac{\sqrt{\mathrm{R}}}{2}\eta\right)\right\}. \tag{11}$$

B. Stability analysis: Modulation equation and associated nonparallel corrections

The perturbation can be expressed, through multiscale analysis, in terms of the stream function as follows:

$$\psi = \varphi(x,y,t;\varepsilon)e^{i\theta(x,t;\varepsilon)}$$
$$= [\varphi_0(x_1,y,t_1) + \varepsilon\varphi_1(x_1,y,t_1) + \cdots]e^{i\theta(x,t;\varepsilon)}. \tag{12}$$

According to the Whitham theory,[22]

$$\partial_x\theta = h_0 = k_0 + is_0, \tag{13}$$

$$\partial_t\theta = -\sigma_0 = -(\omega_0 + ir_0), \tag{14}$$

where $\theta=h_0x-\sigma_0t$; h_0 is the complex dimensionless wave number [$k_0=\mathrm{Re}(h_0)$ wave number, $s_0=\Im(h_0)$ spatial growth rate], while σ_0 is the complex dimensionless pulsation [$\omega_0=\mathrm{Re}(\sigma_0)$ circular frequency, $r_0=\mathrm{Im}(\sigma_0)$ temporal growth rate]. In terms of x_1, t_1, and θ, the spatial and temporal derivatives transform as

$$\partial_x \to h_0\partial_\theta + \varepsilon\partial_{x_1}, \quad \partial_t \to -\sigma_0\partial_\theta + \varepsilon\partial_{t_1}. \tag{15}$$

By applying this transformation to the linearized perturbation equation, a hierarchy of ordinary differential equations, truncated at the first order in ε, is obtained. The zero-order equation is the parametric Orr-Sommerfeld equation, where x_1 and the Reynolds number R are parameters:

$$\mathcal{A}\varphi_0 = \sigma_0\mathcal{B}\varphi_0, \tag{16}$$

$$\varphi_0 \to 0 \quad \text{as } |y| \to \infty, \tag{17}$$

$$\partial_y\varphi_0 \to 0 \quad \text{as } |y| \to \infty, \tag{18}$$

with $\mathcal{A}=\{(\partial_y^2-h_0^2)^2 - ih_0\mathrm{R}[u_0(\partial_y^2-h_0^2)-u_0'']\}$, $\mathcal{B}=-i\mathrm{R}(\partial_y^2-h_0^2)$. It is useful to write $\varphi_0(x_1,t_1,y)=A(x_1,t_1)\zeta_0(x_1,y)$, where A is the spatio-temporal modulation determined at the next order. The eigenvalue problem (16)–(18) becomes

$$\mathcal{A}\zeta_0 = \sigma_0\mathcal{B}\zeta_0, \tag{19}$$

$$\zeta_0 \to 0 \quad \text{as } |y| \to \infty, \tag{20}$$

$$\partial_y\zeta_0 \to 0 \quad \text{as } |y| \to \infty. \tag{21}$$

By numerically solving the zero-order equation and selecting the eigenvalue with the largest imaginary part, a first approximation of the dispersion relation can be obtained: $\sigma_0=\sigma_0(x_1;h_0,\mathrm{R})$. The numerical analysis of this relation yields the loci of the branching points, which are given in Table I. The branching points distribution for $x>3$ has been obtained, in particular, with the help of analytical extrapolations, which are detailed in the Appendix (see also Tables II and III). For a visualization, see the maps drawn in Fig. 2.

The first-order theory gives the nonhomogeneous Orr-Sommerfeld equation, which is parametric in x_1 and R:

$$\mathcal{A}\varphi_1 = \sigma_0\mathcal{B}\varphi_1 + \mathcal{M}\varphi_0, \tag{22}$$

$$\varphi_1 \to 0 \quad \text{as } |y| \to \infty, \tag{23}$$

$$\partial_y\varphi_1 \to 0 \text{ as } |y| \to \infty. \tag{24}$$

The operator

TABLE I. Distribution of the saddle points along the longitudinal coordinate.

x	R=35	R=50	R=100
3.00	$h_0=0.9730-i1.9040$	$h_0=1.3850-i2.2160$	$h_0=2.9000-i1.5960$
	$\sigma_0=1.0194-i0.4861$	$\sigma_0=1.2504-i0.4567$	$\sigma_0=1.5825+i0.1513$
4.10	$h_0=0.4167-i1.7171$	$h_0=0.6254-i2.0754$	$h_0=2.3544-i2.2444$
	$\sigma_0=0.8388-i0.6022$	$\sigma_0=1.0430-i0.6286$	$\sigma_0=1.5138-i0.1695$
5.20	$h_0=0.2242-i1.5156$	$h_0=0.3505-i1.8620$	$h_0=1.6796-i2.5098$
	$\sigma_0=0.6857-i0.6486$	$\sigma_0=0.8681-i0.7067$	$\sigma_0=1.3992-i0.3818$
6.30	$h_0=0.1381-i1.3477$	$h_0=0.2232-i1.6712$	$h_0=1.2244-i2.4207$
	$\sigma_0=0.5769-i0.6597$	$\sigma_0=0.7366-i0.7368$	$\sigma_0=1.2755-i0.5357$
7.40	$h_0=0.0929-i1.2123$	$h_0=0.1547-i1.5125$	$h_0=0.9249-i2.2238$
	$\sigma_0=0.4951-i0.6545$	$\sigma_0=0.6361-i0.7433$	$\sigma_0=1.1537-i0.6304$
9.60	$h_0=0.0500-i1.0129$	$h_0=0.0874-i1.2736$	$h_0=0.5789-i1.8246$
	$\sigma_0=0.3810-i0.6249$	$\sigma_0=0.4951-i0.7254$	$\sigma_0=0.9426-i0.7106$
12.35	$h_0=0.0280-i0.8474$	$h_0=0.0516-i1.0718$	$h_0=0.3657-i1.4590$
	$\sigma_0=0.2917-i0.5794$	$\sigma_0=0.3838-i0.6842$	$\sigma_0=0.7469-i0.7209$
16.20	$h_0=0.0154-i0.6996$	$h_0=0.0301-i0.8895$	$h_0=0.2235-i1.1465$
	$\sigma_0=0.2172-i0.5211$	$\sigma_0=0.2889-i0.6253$	$\sigma_0=0.5645-i0.6888$
22.80	$h_0=0.0075-i0.5537$	$h_0=0.0159-i0.7082$	$h_0=0.1218-i0.8782$
	$\sigma_0=0.1504-i0.4457$	$\sigma_0=0.2001-i0.5447$	$\sigma_0=0.3853-i0.6225$
32.15	$h_0=0.0038-i0.4446$	$h_0=0.0087-i0.5717$	$h_0=0.0675-i0.7166$
	$\sigma_0=0.1058-i0.3766$	$\sigma_0=0.1370-i0.4686$	$\sigma_0=0.2563-i0.5532$
44.80	$h_0=0.0020-i0.3671$	$h_0=0.0051-i0.4743$	$h_0=0.0392-i0.6271$
	$\sigma_0=0.0774-i0.3204$	$\sigma_0=0.0940-i0.4056$	$\sigma_0=0.1692-i0.4951$
59.65	$h_0=0.0012-i0.3170$	$h_0=0.0033-i0.4112$	$h_0=0.0251-i0.5820$
	$\sigma_0=0.0608-i0.2808$	$\sigma_0=0.0672-i0.3609$	$\sigma_0=0.1157-i0.4542$

$$\mathcal{M}=\Big\{\Big[\mathrm{R}(2h_0\sigma_0-3h_0^2u_0-u_0'')+4ih_0^3\Big]\partial_{x_1}+(\mathrm{R}u_0-4ih_0)\partial^3_{x_1yy}-\mathrm{R}v_1(\partial_y^3-h_0^2\partial_y)+\mathrm{R}v_1''\partial_y+ih_0\mathrm{R}\Big[u_1(\partial_y^2-h_0^2)-u_1''\Big]+\mathrm{R}(\partial_y^2-h_0^2)\partial_{t_1}\Big\} \tag{25}$$

is a function of the zero-order dispersion relation and eigenfunction as well as of the base flow; it accounts for entrainment effects through the explicit presence of velocity transversal component v_1. To avoid secular terms in the solution of (22)–(24), the nonhomogeneous term in Eq. (22) should be orthogonal to each solution of the adjoint homogeneous problem. This leads to an evolution equation of modulation A:

TABLE II. Complex wave number interpolating curve of the downstream distribution of the dominant saddle points.

R	$k_0(x)=\Sigma_i c_i^k x^{-i}$	$s_0(x)=\Sigma_i c_i^s x^{-i+1}$
35	$c_1^k=0.0205$, $c_2^k=2.7405$	$c_1^s=-0.1610$, $c_2^s=-9.5190$
	$c_3^k=15.1650$, $c_4^k=8.1000$	$c_3^s=12.8700$
50	$c_1^k=0.1100$, $c_2^k=4.8450$	$c_1^s=-0.2140$, $c_2^s=-12.0660$
	$c_3^k=20.0700$, $c_4^k=5.4000$	$c_3^s=18.1800$
100	$c_1^k=0.7175$, $c_2^k=45.8525$	$c_1^s=-0.0005\times10^3$, $c_2^s=-0.0007\times10^3$
	$c_3^k=38.3850$, $c_4^k=-312.3000$	$c_3^s=-0.2271\times10^3$, $c_4^s=1.2726\times10^3$
		$c_5^s=-1.8436\times10^3$

$$(\partial_{x_1}A)\int_{-\infty}^{\infty}\zeta_0^+\big[M_1+M_2\partial_y^2\big]\zeta_0\mathrm{d}y+(\partial_{t_1}A)\int_{-\infty}^{\infty}\zeta_0^+\big[M_7+M_8\partial_y^2\big]\zeta_0\mathrm{d}y+A\int_{-\infty}^{\infty}\zeta_0^+\big[M_1\partial_{x_1}+M_2\partial^3_{x_1yy}+M_3+M_4\partial_y+M_5\partial_y^2+M_6\partial_y^3\big]\zeta_0\mathrm{d}y=0, \tag{26}$$

where the coefficients M_j are

$$M_1=\mathrm{R}(2h_0\sigma_0-3h_0^2u_0-u_0'')+4ih_0^3, \tag{27}$$

$$M_2=\mathrm{R}u_0-4ih_0, \tag{28}$$

$$M_3=-ih_0\mathrm{R}(\partial_y^2+h_0^2)u_1, \tag{29}$$

$$M_4=-\mathrm{R}(\partial_y^2+h_0^2)v_1, \tag{30}$$

$$M_5=ih_0\mathrm{R}u_1, \tag{31}$$

$$M_6=\mathrm{R}v_1, \tag{32}$$

$$M_7=-\mathrm{R}h_0^2, \tag{33}$$

$$M_8=\mathrm{R}, \tag{34}$$

TABLE III. Complex pulsation interpolating curve of the downstream distribution of the dominant saddle points.

R	$\omega_0(x)=\Sigma_i c_i^\omega x^{-i+1}$	$r_0(x)=\Sigma_i c_i^r x^{-i+1}$
	$c_1^\omega=0.0187$, $c_2^\omega=2.0880$	$c_1^r=-0.1403$, $c_2^r=-9.4102$
35	$c_3^\omega=28.5906$, $c_4^\omega=-201.5260$	$c_3^r=65.0415$, $c_4^r=-230.5392$
	$c_5^\omega=601.3316$, $c_6^\omega=-688.1536$	$c_5^r=472.4563$, $c_6^r=-420.4417$
	$c_1^\omega=-0.0114$, $c_2^\omega=4.5533$	$c_1^r=-0.1999$, $c_2^r=-10.8650$
50	$c_3^\omega=9.1532$, $c_4^\omega=-78.4682$	$c_3^r=79.9060$, $c_4^r=-285.3133$
	$c_5^\omega=205.6623$, $c_6^\omega=-220.1156$	$c_5^r=576.7085$, $c_6^r=-502.1086$
	$c_1^\omega=0.0000$, $c_2^\omega=0.0081\times10^3$	$c_1^r=-0.0003\times10^3$, $c_2^r=-0.0092\times10^3$
100	$c_3^\omega=0.0531\times10^3$, $c_4^\omega=-0.5530\times10^3$	$c_3^r=0.0405\times10^3$, $c_4^r=0.2403\times10^3$
	$c_5^\omega=1.6819\times10^3$, $c_6^\omega=-1.7701\times10^3$	$c_5^r=-1.5176\times10^3$, $c_6^r=2.1540\times10^3$

and ζ_0^+ is the perturbation stream function of the homogeneous adjoint problem. If the multiscale analysis is only based on the slow spatial evolution of the system, coefficients M_7, M_8 do not exist and the modulation equation is simply $\mathrm{d}_{x_1}A(x_1)=ih_1(x_1)A(x_1)$, where h_1 is a function of M_i, and $i=1,\ldots,6$.[16] By substituting $A(x_1,t_1)$ with $e^{a(x_1,t_1)}$, following Bouthier[17] and going back to the original coordinates x and t, Eq. (26) can be written as

$$\partial_t a + p(x)\partial_x a + \varepsilon q(x) = 0, \tag{35}$$

where coefficients

$$p(x) = \frac{\int_{-\infty}^{\infty} \zeta_0^+[M_1 + M_2\partial_y^2]\zeta_0 \mathrm{d}y}{\int_{-\infty}^{\infty} \zeta_0^+[M_7 + M_8\partial_y^2]\zeta_0 \mathrm{d}y} \tag{36}$$

and

$$q(x) = \frac{\int_{-\infty}^{\infty} \zeta_0^+[M_1\partial_{x_1} + M_2\partial^3_{x_1yy} + M_3 + M_4\partial_y + M_5\partial_y^2 + M_6\partial_y^3]\zeta_0 \mathrm{d}y}{\int_{-\infty}^{\infty} \zeta_0^+[M_7 + M_8\partial_y^2]\zeta_0 \mathrm{d}y} \tag{37}$$

are not singular.

The modulation equation can be solved numerically by specifying the initial and boundary conditions. The considered spatial domain extends from a few body-scales D downstream from the body to the far field (in the present computations, $x_i<x<x_f$, where $x_i=3$ and $x_f=60$). Since only one boundary condition has to be imposed, modulation is required to satisfy the asymptotic uniformity in the far field $x=x_f$; that is, the Neumann condition

$$(\partial_x a)_{x=x_f} = 0, \quad \forall\, t, \tag{38}$$

while a natural choice for the initial condition is

$$a_{x,t=0} = (\text{const})(1+i). \tag{39}$$

Considering that $\varphi_1(x_1,y,t_1)=A(x_1,t_1)\zeta_1(x_1,y)$, and that the complete solution (order 0+order 1) is

$$\begin{aligned}\psi &= (\varphi_0 + \varepsilon\varphi_1)e^{i\theta} = A(x_1,t_1)(\zeta_0 + \varepsilon\zeta_1)e^{i\theta} \\ &= (\zeta_0 + \varepsilon\zeta_1)e^{i\theta + i\theta_1},\end{aligned} \tag{40}$$

the complete phase becomes $\Theta=\theta+\theta_1$, where $a=i\theta_1$. Due to the multiscaling, the wave number is $h=\partial\Theta/\partial x=h_0\partial\Theta/\partial\theta+\varepsilon\partial\Theta/\partial x_1=h_0+\varepsilon\partial\theta_1/\partial x_1$ and the pulsation is $\sigma=-\partial\Theta/\partial t=-\sigma_0\partial\Theta/\partial\theta+\varepsilon\partial\theta_1/\partial t_1=-\sigma_0+\varepsilon\partial\theta_1/\partial t_1$. The first-order corrections of the instability characteristics are thus obtained as

$$h_1 = \partial\theta_1/\partial x_1 = k_1 + is_1, \quad \sigma_1 = -\partial\theta_1/\partial t_1 = \omega_1 + ir_1. \tag{41}$$

C. Perturbation hypothesis: Saddle point sequence

Coefficients $p(x)$ and $q(x)$ of the modulation equation (35) are functions of the disturbance and of the base flow. The base flow is only present in p through the zero-order longitudinal velocity u_0, while the first-order longitudinal and transversal velocities u_1 and v_1 are instead present in q. The distributions of the real and imaginary parts of coefficients p and εq can be computed by inserting in h_0 and σ_0 the values of the dominant saddle point of the zero-order dispersion relation taken at each x position along the wake. These distributions are shown in Fig. 3 for R=35, 50, and 100.

In so doing, the disturbance is locally tuned, through the modulation function, to the property of the instability as can be seen from the zero-order theory (near-parallel parametric Orr-Sommerfeld treatment). This leads to a synthetic analysis of the nonparallel correction on the instability characteristics. In such a way, the parametrization with respect to the longitudinal position in the wake, as applied in Belan and Tordella[23] (see Fig. 5), is not necessary since the evolution of the zero-order dispersion relation is directly inserted into the variable coefficients of the modulation equation. The streamwise variation of the instability characteristics is deduced from the spatial and temporal derivatives of the modulation function. With this approach, the system is considered as locally perturbed by waves with a wave number that varies along the wake and which is equal to the wave number of the dominant saddle point of the zero-order dispersion relation, taken at different Reynolds numbers. Since the perturbation is no more parameterized with respect to a given wave number, the Reynolds number remains the only parameter of the present stability analysis.

III. RESULTS

The first-order correction of the instability characteristics is obtained through relation (41), after having solved the modulation equation (35) and the associated auxiliary conditions, (38) and (39). It can be seen, in Fig. 4, that the correction of the characteristics values—at the saddle points—increases with the Reynolds number. At the subcritical

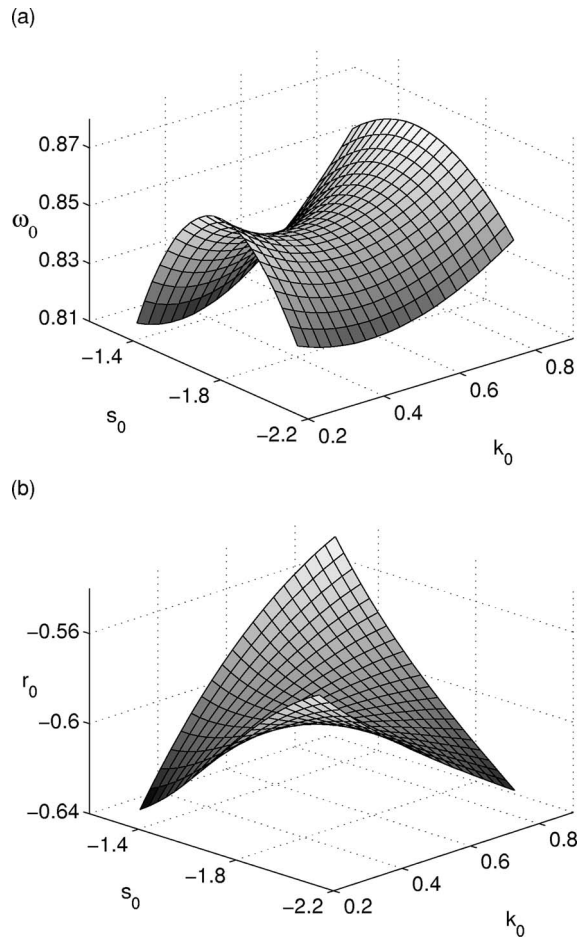

FIG. 2. Multidimensional map: (a) ω_0 (k_0,s_0) and (b) r_0 (k_0,s_0); R=35, $x/D=4$.

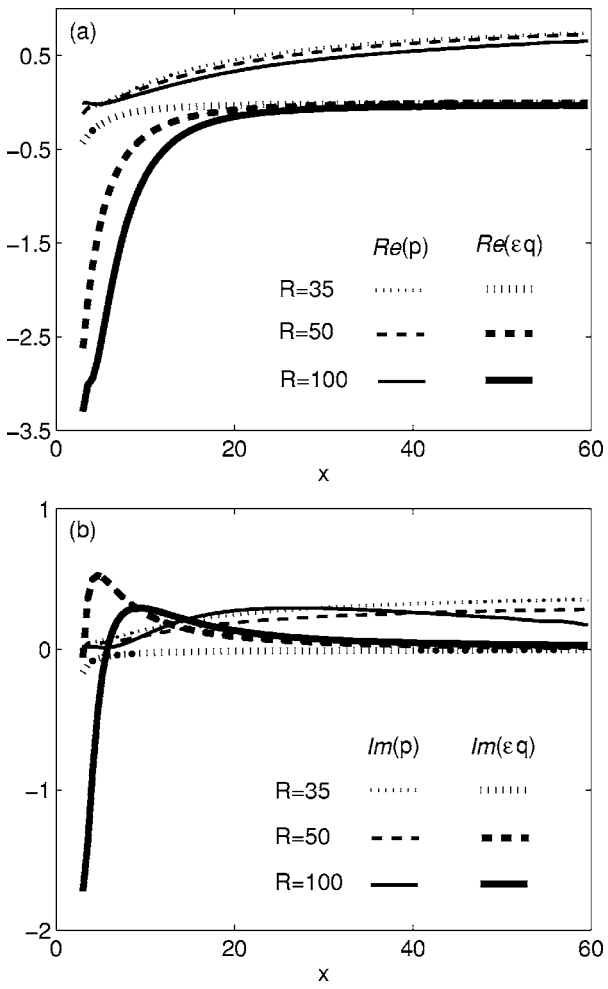

FIG. 3. Real (a) and imaginary (b) part of the modulation equation coefficients.

Reynolds number (R=35), the lowest value here considered, the correction is negligible throughout the intermediate and far domains. Another general feature, which is Reynolds number independent, is the vanishing of the first-order correction as $x\to\infty$. In the first part of the intermediate wake, $3<x<20$, the multiscaling correction instead increases the values of all the four characteristics, which results in a reduction of the spatial growth rate modulus [see Fig. 4(b)].

The largest variations between the complete and the zero-order results are shown by the pulsation ω and the temporal growth factor r [see Figs. 4(c) and 4(d)]. In fact, for these quantities, corrections of the order of 50–100% can be observed in the first 15 diameters downstream to the body. At R=100, the complete pulsation exhibits a point of relative maximum for $x\sim 7$. The temporal growth factor r becomes positive, for both R=50 and 100, in the first part of the intermediate wake region. Thus, at these Reynolds numbers, absolute instability pockets appear which extend to $x\sim 7$ and $x\sim 10$, respectively.

Figure 5 shows a comparison of the results obtained with the present perturbation hypothesis and the results obtained by considering the system disturbed by a wave with a complex wave number that is kept constant downstream to the wake,[23] and equal to the zero-order value shown at the saddle point in $x=4.10$ [see Figs. 5(a) and 5(b)]. One can see that the two-perturbation hypothesis yield the same results close to $x=4.10$, but differ downstream, where, in the latter case, the perturbation is no longer locally tuned to the more unstable wave number, which results in forcing of the system to the chosen wave number in the positions of the wake that are different from $x=4.10$. A similar behavior is observed if the position of the forcing point is moved along the wake. It can thus be concluded that the present perturbation, being tuned to the natural sequence along the longitudinal coordinate of the proper wave numbers, is an efficient tool to highlight the evolution of the stability properties in the intermediate wake.

Data from the global results obtained by Pier[10] (direct numerical simulations), Williamson[21] (laboratory observations), and Zebib[3] (numerical experiments) are included in Fig. 6. In this figure, the x positions pointed out represent the wake section, where the longitudinal distribution of pulsation obtained with the present method match the global pulsation obtained in these numerical and laboratory experiments. A linear interpolation on the points we have determined shows that the experimental data fall within an accuracy of ±5% around a pulsation curve that grows with the Reynolds number.

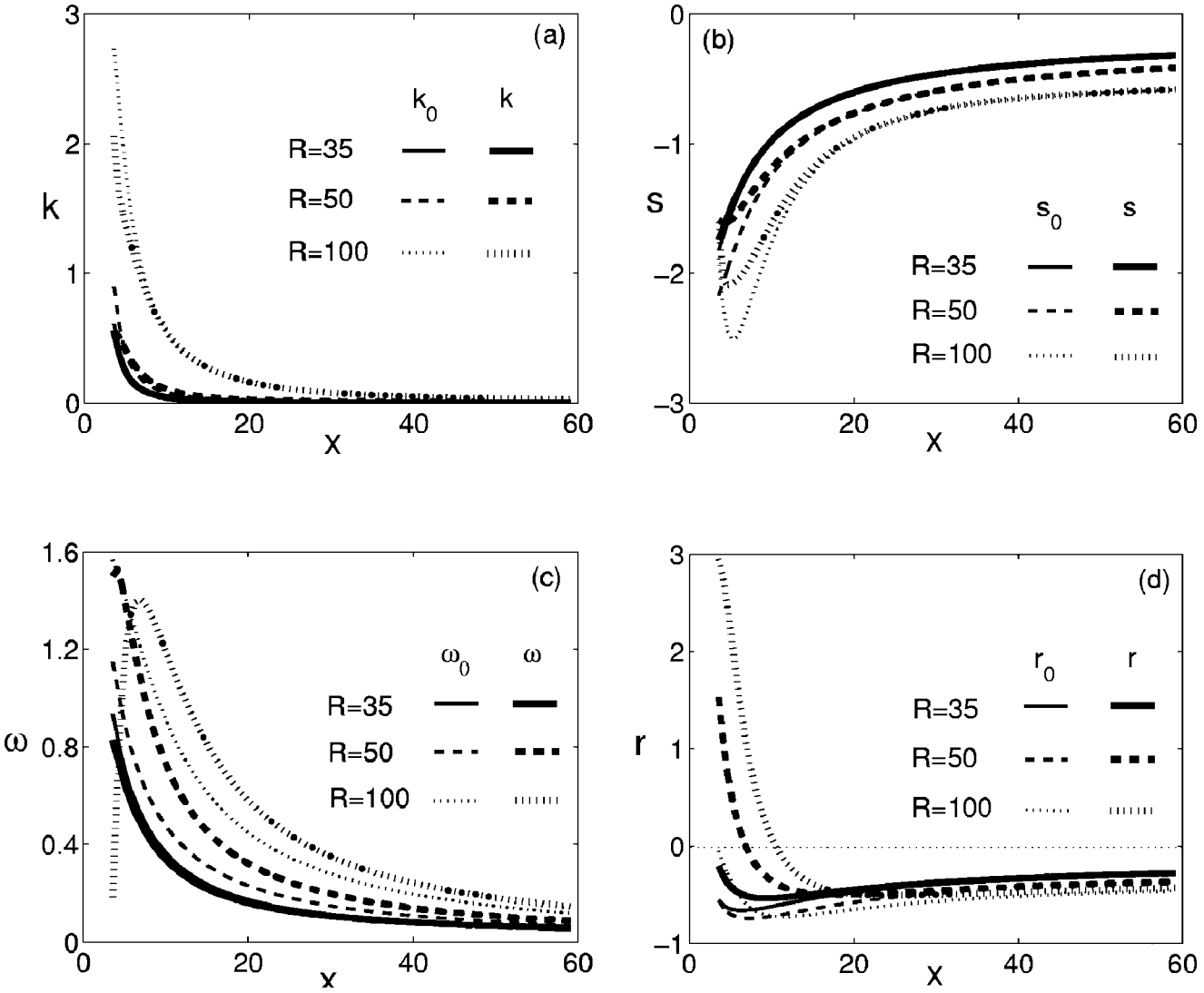

FIG. 4. Instability characteristics: (a) wave number, (b) spatial growth rate, (c) pulsation, and (d) temporal growth rate; R=35, 50, and 100.

This stability analysis yields marginal conditions of stability for the asymptotic far wake (see Figs. 4 and 7).

IV. EIGENFUNCTION AND EIGENVALUE ASYMPTOTIC THEORY

This section shows how it is possible to obtain the asymptotic behavior of the instability characteristics $k_0, \omega_0, \sigma_0, r_0$ from the properties of the Orr-Sommerfeld problem in the limit $x \sim \infty$.

The present nonparallel stability analysis shows that the saddle point wave numbers k_0 decay rapidly as $x \sim \infty$. Thus, we can assume this decay as a hypothesis of behavior of the solutions of Eq. (19). In the same equation, the base flow appears together with its second y derivative; the relevant asymptotic forms are

$$u_0 = 1 + x^{-1/2}\phi_1(yx^{-1/2}) + O(x^{-1}) = 1 - \frac{\tilde{c_D}}{e^{\mathrm{R}y^2/4x}\sqrt{x}} + O(x^{-1}) = O(1), \tag{42}$$

$$\partial_y^2 u_0 = \frac{\tilde{c_D}\mathrm{R}}{2e^{\mathrm{R}y^2/4x}x^{3/2}} - \frac{\tilde{c_D}\mathrm{R}^2y^2}{4e^{\mathrm{R}y^2/4x}x^{5/2}} + O(x^{-7/2}) = O(x^{-3/2}). \tag{43}$$

Clearly, $\partial_y^2 u_0$ is negligible in comparison to u_0; therefore, operator $\mathcal{A}$, which is present in (16) and (19), becomes

$$\mathcal{A} = \{(\partial_y^2 - h_0^2)^2 - ih_0\mathrm{R}u_0(\partial_y^2 - h_0^2)\}. \tag{44}$$

Now the eigenvalue problem (19) with the relevant boundary conditions can be rewritten in the form

$$\{\partial_y^2 - h_0^2 - ih_0\mathrm{R}u_0\}f = -i\mathrm{R}\sigma_0 f, \tag{45}$$

$$f \to 0 \text{ as } |y| \to \infty, \tag{46}$$

where

$$f(x,y) = (\partial_y^2 - h_0^2)\varphi_0(x,y). \tag{47}$$

It is useful to rewrite the base flow in the form $u_0 = 1 + g(x,y)$, where $g(x,y) = -\tilde{c_D}x^{-1/2}e^{-\mathrm{R}y^2/4x}$ is the well-known asymptotic Gaussian law for velocity defect in the wakes.

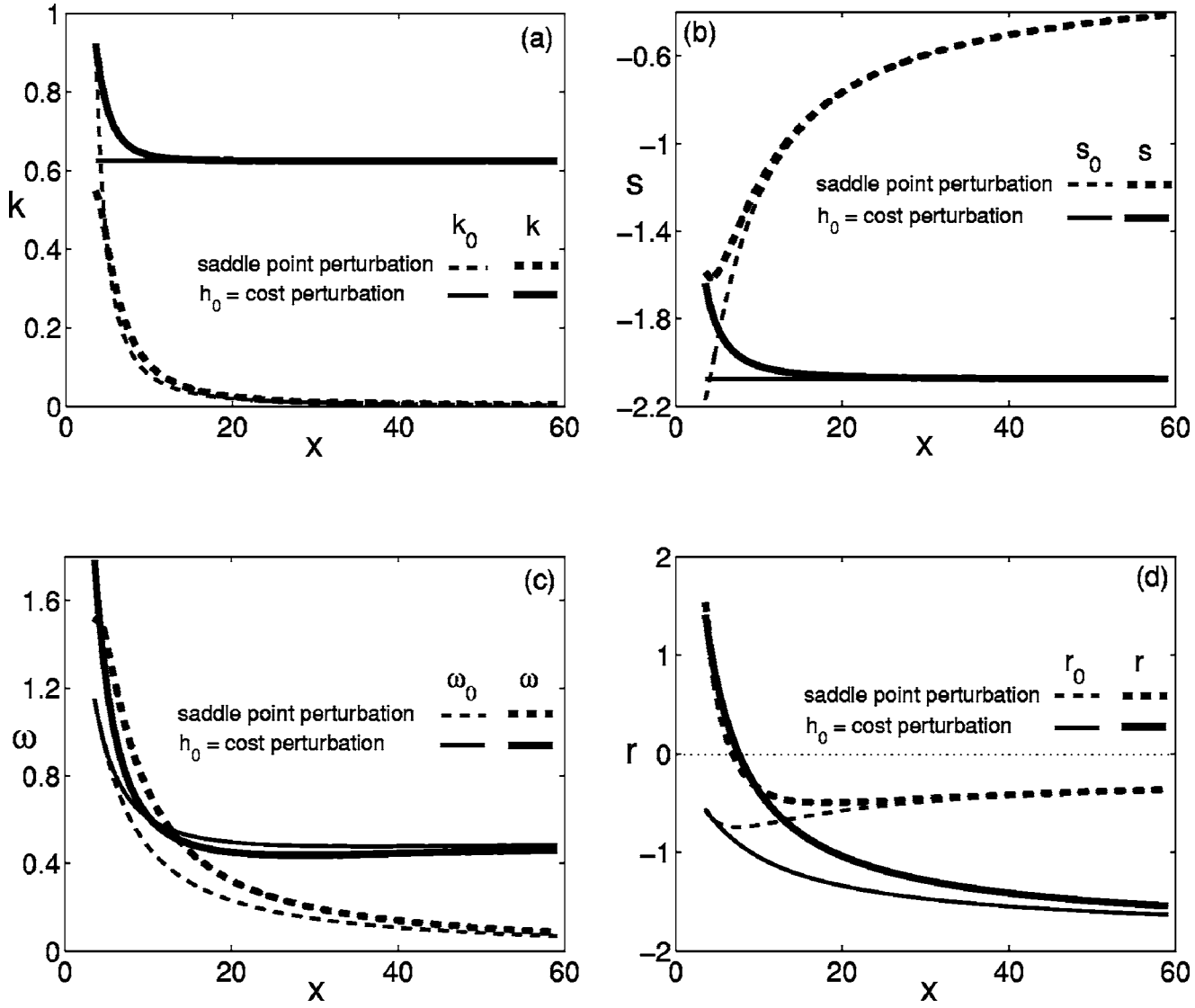

FIG. 5. Comparison between the instability characteristics with the present perturbation hypothesis (spatial sequence of saddle points) and the perturbation with h_0 (x=4.10)=const at R=50: (a) wave number, (b) spatial growth rate, (c) pulsation, and (d) temporal growth rate.

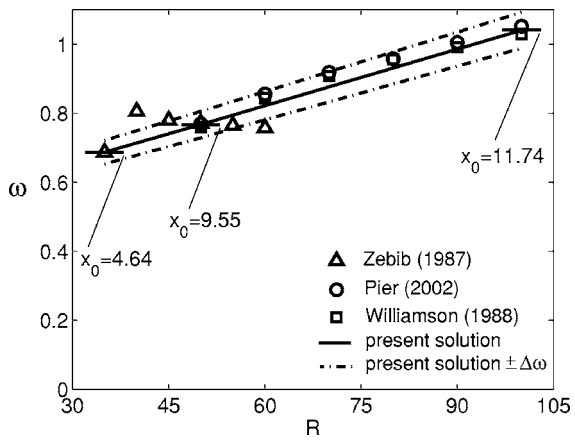

FIG. 6. Comparison between the global pulsation data according to Pier (Ref. 10), Zebib (Ref. 3), Williamson (Ref. 21), and present solution (accuracy $\Delta\omega$=0.05).

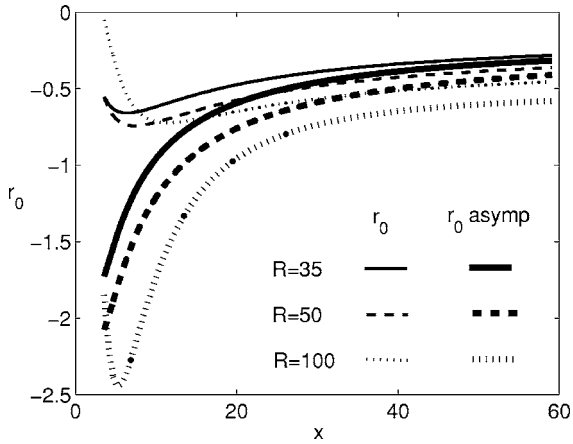

FIG. 7. Temporal growth rate, $r_0(x)$. Comparison between the asymptotic behavior $r_0=s_0(x)+s_0(x)^2$/R and present solution at order zero (extrapolated curve, see Appendix); R=35, 50, and 100.

Parameter $P=ih_0\mathrm{R}$ and the generalized eigenvalue $w=i\mathrm{R}\sigma_0 - ih_0\mathrm{R}-h_0^2$ are also introduced. The eigenvalue problem (45) finally becomes

$$(-\partial_y^2 + Pg)f = wf, \tag{48}$$

with the same boundary conditions. In this equation, $P=ih_0\mathrm{R}\sim -s_0\mathrm{R}$ is a real parameter according to the hypothesis $k_0\sim 0$. One can observe that (48) is the stationary Schrödinger equation. Moreover, if we assume $s_0<0$, in agreement with the numerical results described in Sec. III, positive values are obtained for the P parameter. Product $Pg(x,y)$ at a given x is therefore a negative function throughout, that vanishes as $|y|\to\infty$; this makes the eigenvalue problem (48) become the famous one-dimensional "potential well" problem, which has been widely treated in theoretical physics (see, for example, Messiah[24]).

Some properties of this problem should be mentioned at this point: the operator in (48) is self-adjoint; thus, the eigenvalues w are real. The eigenvalue spectrum has a discrete part $\{w_0,w_1,w_2,\ldots\}$, and all these eigenvalues satisfy the inequality

$$g_{\min} < w_n < 0, \tag{49}$$

where $g_{\min}=-\tilde{c_D}x^{-1/2}$ is the axial value of g (wake center).

These properties lead to interesting consequences. First, since w is real,

$$\mathrm{Im}\{w\} = \mathrm{Im}\{i\mathrm{R}\sigma_0 - ih_0\mathrm{R} - h_0^2\} = -k_0(\mathrm{R}+2s_0) + \mathrm{R}\omega_0 = 0, \tag{50}$$

so that $k_0\sim 0$ implies

$$\omega_0 \sim 0; \tag{51}$$

that is, if the saddle point wave numbers k_0 vanish rapidly, the pulsation ω_0 should also vanish rapidly. This result is in good agreement with the present numerical computations (see Fig. 3).

Furthermore, the inequality (49) shows that

$$g_{\min} < -r_0\mathrm{R} + s_0(\mathrm{R}+s_0) < 0; \tag{52}$$

however, in the limit $x\sim\infty$, we know that $g_{\min}\to 0$, thus, $-r_0\mathrm{R}+s_0(\mathrm{R}+s_0)\sim 0$ and a relation can be found between the asymptotic behavior of the temporal and spatial growth factors:

$$r_0 \sim s_0 + s_0^2/\mathrm{R}. \tag{53}$$

Since finite values for an asymptotic uniform flow at infinity are unphysical, because uniformity means absence of spatial and temporal scales, and since positive infinite values for r_0 are *a priori* excluded, it can be deduced that both $r_0, s_0\to 0$.

This result is in good agreement with the numerical computations, as shown in Fig. 3, where the computations are compared with the simple curve $r_0=s_0+s_0^2/\mathrm{R}$ (unitary proportionality constant).

V. CONCLUSIONS

The spatially varying disturbance we have used here to represent the amplitude modulation proves to be a synthetic way of highlighting the behavior of the convective instability in the intermediate bluff body wake. This disturbance is tuned to the local physical wave numbers along the wake and is associated to a classical spatial and temporal Wentzel-Kramers-Brillouin-Jeffreys (WKBJ) analysis carried out on a basic flow previously derived from intermediate asymptotics. The multiscaling explicitly accounts for the effects associated to the lateral momentum dynamics, at a given Reynolds number. The first-order correction allows absolute instability pockets to be determined in the first part of the intermediate wake. These pockets are present when the Reynolds number R is equal to 50 and 100, but are absent when R is as low as 35. This is in general agreement with the standard notion of a critical Reynolds number of about 47 for the onset of the first observable instability.

The size of the correction increases with R and is larger for the pulsation and the temporal growth factor than for the spatial growth factor. It is negligible for the wave number.

The pulsation variation with R of the point in the wake where the temporal growth factor is almost equal to zero is in good agreement with experimental global flow data in literature. Another outcome of the present study is that the convective instability asymptotically holds a condition of marginal stability. All the four instability characteristics vanish at infinity downstream to the body creating the wake flow.

The far-wake asymptotic behavior shown by this WKBJ analysis has also been independently obtained through an analysis based on the properties of the Orr-Sommerfeld problem.

APPENDIX: STREAMWISE DISTRIBUTION OF THE INSTABILITY CHARACTERISTICS AT SADDLE POINTS: INTERPOLATION CURVES

As the Orr-Sommerfeld problem (19)–(21) solution is necessarily computed on a numerical bounded domain instead of on the theoretical unbounded one, the determination of the saddle points is sensitive to the extension of the actual numerical domain and to the number and choice of the collocation points.

Moreover, problems arise when small values of k_0 are reached because singularities are present on the s_0 axis in the complex wave number plane. This aspect becomes important at just a few diameters behind the cylinder, since the wave number rapidly decreases with the longitudinal coordinate x.

For these reasons, by minimizing the relative error between the data and the interpolating curve, truncated Laurent series have been used to extrapolate the saddle point behavior from data at the lower x values. These data are more accurate, because the values of k_0 are not too small at these longitudinal stations. The curves obtained are in agreement with the far field asymptotics (see Sec. IV and Fig. 7).

Assuming that k_0 is non-negative, its extrapolating function is $k_0(x)=\Sigma_i c_i^k x^{-i}$, $i=1,2,\ldots$. For the other stability characteristics (s_0, ω_0, r_0), the extrapolating functions are $s_0(x)=\Sigma_i c_i^s x^{-i+1}$, $\omega_0(x)=\Sigma_i c_i^\omega x^{-i+1}$, $r_0(x)=\Sigma_i c_i^r x^{-i+1}$, $i=1,2,\ldots$.

The Laurent series coefficients for the stability characteristics are given in Tables II and III for R=35, 50, and 100. The domain of validity is $3<x<60$.

[1] G. E. Mattingly, Jr. and W. O. Criminale, "Disturbance characteristics in a plane jet," Phys. Fluids **14**, 2258 (1971).
[2] G. E. Mattingly, Jr. and W. O. Criminale, "The stability of an incompressible two-dimensional wake," J. Fluid Mech. **51**, 233 (1972).
[3] A. Zebib, "Stability of viscous flow past a circular cylinder," J. Eng. Math. **21**, 155 (1987).
[4] G. S. Triantafyllou, K. Kupfer, and A. Bers, "Absolute instabilities and self-sustained oscillations in the wake of circular cylinders," Phys. Rev. Lett. **59**, 1914 (1987).
[5] P. Huerre and P. A. Monkewitz, "Local and global instabilities in spatially developing flows," Annu. Rev. Fluid Mech. **22**, 473 (1990).
[6] H. Oertel, "Wakes behind blunt bodies," Annu. Rev. Fluid Mech. **22**, 539 (1990).
[7] P. A. Monkewitz, "The absolute and convective nature of instability in two-dimensional wakes at low Reynolds numbers," Phys. Fluids **31**, 999 (1988).
[8] X. Yang and A. Zebib, "Absolute and convective instability of a cylinder wake," Phys. Fluids A **1**, 689 (1989).
[9] K. Hannemann and H. Oertel, "Numerical simulation of the absolutely and convectively unstable wake," J. Fluid Mech. **199**, 55 (1989).
[10] B. Pier, "On the frequency selection of finite-amplitude vortex shedding in the cylinder wake," J. Fluid Mech. **458**, 407 (2002).
[11] J. M. Chomaz, P. Huerre, and L. G. Redekopp, "A frequency selection criterion in spatially developing flows," Stud. Appl. Math. **84**, 119 (1991).
[12] P. A. Monkewitz, P. Huerre, and J. M. Chomaz, "Global linear-stability analysis of weakly nonparallel shear flows," J. Fluid Mech. **251**, 1 (1993).
[13] B. Pier and P. Huerre, "Nonlinear self-sustained structures and fronts in spatially developing wake flows," J. Fluid Mech. **435**, 145 (2001).
[14] L. S. Hultgren and A. K. Aggarwal, "Absolute instability of the Gaussian wake profile," Phys. Fluids **30**, 3383 (1987).
[15] P. J. Schmid and D. S. Henningson, *Stability and Transition in Shear Flows* (Springer, New York, 2001).
[16] D. Tordella and M. Belan, "On the domain of validity of the near-parallel combined stability analysis for the 2D intermediate and far bluff body wake," Z. Angew. Math. Mech. **85**, 51 (2005).
[17] M. Bouthier, "Stabilité linéare des écoulements presque parallèles," J. Mec. **11**, 599 (1972).
[18] G. I. Barenblatt, *Scaling, Self-similarity, and Intermediate Asymptotics* (Cambridge University Press, Cambridge, UK, 1996), preface, p. xiii.
[19] D. Tordella and M. Belan, "A new matched asymptotic expansion for the intermediate and far flow behind a finite body," Phys. Fluids **15**, 1897 (2003).
[20] M. Belan and D. Tordella, "Asymptotic expansions for two-dimensional symmetrical laminar wakes," Z. Angew. Math. Mech. **82**, 219 (2002).
[21] C. Williamson, "Defining a universal and continuous Strouhal-Reynolds number relationship for the laminar vortex shedding of a circular cylinder," Phys. Fluids **31**, 2742 (1988).
[22] G. B. Whitham, *Linear and Nonlinear Waves* (John Wiley & Sons, New York, 1974).
[23] M. Belan and D. Tordella, "Convective instability in wake intermediate asymptotics," J. Fluid Mech. **552**, 127 (2006).
[24] A. Messiah, *Mecanique Quantique* (Dunod, Paris, 1960).